Pharm Res (2012) 29:69–82
DOI 10.1007/s11095-011-0511-9

RESEARCH PAPER

Encapsulation and Release of Amphotericin B from an ABC Triblock Fluorous Copolymer

Jun-Pil Jee • Aaron McCoy • Sandro Mecozzi

Received: 2 May 2011 / Accepted: 10 June 2011 / Published online: 8 July 2011

ABSTRACT

Purpose PEG-phospholipid-based micelles have been successfully used for the solubilization of several hydrophobic drugs but generally lack sustained stability in blood. Our novel PEG-Fluorocarbon-DSPE polymers were designed to increase stability and improve time-release properties of drug-loaded micelles.

Methods Novel ABC fluorous copolymers were synthesized, characterized, and used for encapsulation release of amphotericin B. FRET studies were used to study micelle stability.

Results The micelles formed by the new polymers showed lower critical micelle concentrations and higher viscosity cores than those formed by the polymers lacking the fluorous block. FRET studies indicated that fluorocarbon-containing micelles had increased stability in presence of human serum. Physicochemical properties and *in vitro* release profile of micelles loaded with Amphotericin B (AmB) were studied.

Conclusions The effect of PEG length and fluorocarbon incorporation were investigated. The shorter hydrophilic PEG2K induced greater stability than PEG5K by decreasing the proportion of hydrophilic block of the polymer. The fluorocarbon placed between hydrophilic and hydrophobic block formed a fluorous shell contributing to the enhanced thermodynamic stability of micelles and to the drug sustained release. Polymer mPEG2K-F_{10}-DSPE, bearing both a fluorocarbon block and a shorter mPEG, showed the greatest stability and the longest half-life for AmB release.

KEY WORDS Amphotericin B · drug delivery · fluorous · polymeric micelle · stability

ABBREVIATIONS

AmB	Amphotericin B
CMC	critical micelle concentration
$DiIC_{18}(3)$	1,1-dioctadecyl-3,3,3,3-tetramethylindocarbocyanine perchlorate
$DiOC_{18}(3)$	3,3-dioctadecyloxacarbocyanine perchlorate
DSPE	1,2-distearoyl-sn-glycero-3-phosphoethanolamine
FRET	Förster resonance energy transfer
mPEG	methoxy-capped poly(ethylene glycol)
P3P	1,3-(1,1′-dipyrenyl) propane
PEG	poly(ethylene glycol)
PEG2K	poly(ethylene glycol) of an average molecular weight of 2,000
PEG5K	poly(ethylene glycol) of an average molecular weight of 5,000

INTRODUCTION

Amphiphilic block copolymers that assemble into micelles or liposomes in aqueous solutions are commonly studied in the field of drug delivery. Micelle-based drug delivery systems made from amphiphilic block copolymers, which self-assemble into structures with hydrophobic cores and hydrophilic exteriors, have proven to be an attractive method of delivering poorly soluble drugs (1,2). The hydrophobic drug

J.-P. Jee · A. McCoy · S. Mecozzi
School of Pharmacy, University of Wisconsin-Madison
1101 University Avenue
Madison, Wisconsin 53706, USA

A. McCoy · S. Mecozzi
Department of Chemistry, University of Wisconsin-Madison
1101 University Avenue
Madison, Wisconsin 53706, USA

S. Mecozzi (✉)
School of Pharmacy, University of Wisconsin-Madison
777 Highland Avenue
Madison, Wisconsin 53705, USA
e-mail: smecozzi@wisc.edu

can be encapsulated in the core while the hydrophilic portion provides the necessary water solubility for the system. This allows the solubilization of sparingly soluble drugs as well as an increase in bioavailability. Poly(ethylene glycol), PEG, has been the most common hydrophilic block because of its ability to be strongly hydrated, its high conformational flexibility, and its remarkable biocompatibility (2). The inner hydrophobic block has shown greater variability depending on the system being studied, but phospholipids such as DSPE have been extensively studied (3–6).

The stability of a micelle, measured by its critical micelle concentration (CMC), is an important consideration in drug delivery systems (7). Aggregates with relatively high CMCs, such as low-molecular-weight surfactants, are unstable upon strong dilution, such as during intravenous administration into the bloodstream. Polymeric micelles are characterized by greater thermodynamic stability, as evident by lower CMCs, than smaller surfactants. However, in order for a micelle to be successful as a delivery vessel, it must be kinetically stable in the presence of blood proteins, such as albumin. Dissociation due to binding by hydrophobic blood proteins has been shown to be the main mechanism with which micelles are dissociated in the bloodstream; moreover, recent studies have shown that poly(ethylene glycol)-*block*-poly(caprolactone) and poly(ethylene glycol)-*block*-poly(D,L-lactic acid) micelles lose their integrity in serum mimicking conditions (8,9). An additional concern raised in some release studies of physically entrapped drugs is the sudden release, or burst, of drugs once the micelle reaches the tumor (10). A slower, sustained release of the drug from the conjugate micelles can result in a prolonged effect period against cancer cells, reduce the required amount of drug, and even depress toxic side effects in humans (11). Chemical cross-linking of either the exterior shell or the core-shell interface or the micelle core has been investigated for the purpose of increasing the stability of polymer micelles in blood (12–15). However, the complexity of cross-linking processes, the possible degeneration of loaded drugs during cross-linking processes, and drug release problems due to the cross-linked core limit the wide application of these methodologies (12). Increasing the hydrophobicity of the interior of the micelle normally leads to lower CMCs, indicating greater thermodynamic stability, and thus slower drug release, while a polymer resistant to blood protein binding will show increased circulation.

Since hydrophobic blocks are required to obtain stable micelles, we decided to explore the incorporation of perfluorocarbons into drug delivery systems. Fluorous compounds are characterized by both lipophobicity and extreme hydrophobicity, also known as fluorophilicity (16). Fluorocarbons tend to be chemical and biologically inert, have high gas solubilities, and show a strong tendency to form highly stable self-assemblies (17). Fluorocarbons have been investigated for oxygen transport, using neat perfluorooctyl bromide (18) and using fluorocarbon-based emulsions (19,20). Numerous fluorinated colloids have been investigated as drug delivery systems, using fluorocarbon emulsions stabilized by fluorocarbon-hydrocarbon diblocks as the surfactant (21). Recent studies have used fluorocarbon emulsions as delivery vessels using *in vivo* monitoring of the delivery system by ^{19}F MRI (22). It is noteworthy to point out that a fluorous segment should not participate in the encapsulation of hydrophobic drugs due to the lipophobic properties of the fluorocarbon. Incorporation of fluorous segments into polymeric micelles should enhance thermodynamic stability by increasing hydrophobicity of the micelle core, while kinetic stability will be enhanced by the lipophobic fluorous segment by reduced binding to blood proteins.

The model drug chosen for this study was the hydrophobic antifungal Amphotericin B (AmB), as similar PEG-Phospholipid systems have incorporated AmB and shown moderate success (23–25). AmB is the drug of choice for treating systemic fungal infections (26). However, its poor water solubility and systemic toxicity have limited its clinical effectiveness (27). AmB toxicity is likely related to the relative aggregation state of the drug (28–31). Liposomal and micellar formulations have been shown to encapsulate and disaggregate AmB (25,32). Slow, sustained release of monomeric AmB would be beneficial, as clinical research has shown a continuous infusion of AmB over 24 h is better tolerated than a standard 2–4 h infusion (33–36). Additionally, dose-related nephrotoxicity of AmB has been shown to limit higher dosages or longer durations of therapy (37).

In this study, we have synthesized novel micelle-forming amphiphilic block copolymers, mPEG2K-F_{10}-DSPE and mPEG5K-F_{10}-DSPE, and characterized their physicochemical properties. We have prepared micelles of these polymers and the commercially available mPEG2K-DSPE and mPEG5K-DSPE and explored the encapsulation and release properties of AmB from these polymers. Micelle stability was examined in buffer and in human serum.

MATERIALS AND METHODS

Materials

AmB was purchased from Alpharma (Copenhagen, Denmark). 1,2-distearoyl-sn-glycero-3-phosphoethanolamine (DSPE), 1,2-distearoyl-sn-glycero-3-phosphoethanolamine-N-[methoxy (polyethylene glycol)-2000] (mPEG2K-DSPE) and 1,2-distearoyl-sn-glycero-3-phosphoethanolamine-N-[methoxy(polyethylene glycol)-5000] (mPEG5K-DSPE) were purchased from Avanti Polar Lipids Inc. Polyethylene glycol monomethyl ether with average molecular weights of 2,000 and 5,000 (mPEG2K and mPEG5K respectively) were purchased from Sigma Aldrich

(St. Louis, MO, USA) (Alabaster, AL, USA). 1,3-(1,1′-dipyrenyl) propane (P3P) was obtained from Invitrogen (Eugene, OR, USA). 1H,1H,12H,12H-Perfluoro-1,12-dodecanediol was purchased from SynQuest Laboratories Inc. (Alachua, FL). Human serum was obtained from Innovative Research (Novi, MI, USA). All solvents were of ACS grade or higher and were purchased from Sigma-Aldrich Inc. (St. Louis, MO, USA) or Fisher Scientific (Hanover Park, IL, USA). All other reagents were purchased from Sigma Aldrich Co. (St. Louis, MO, USA) and used as received, unless otherwise mentioned. Chromatographic separations were performed using Silicycle 60Å SiO_2. Fluorous separations used Fluoro-Flash® 40 μm silica. ^1H and ^{19}F NMR spectra were obtained on Varian VI-400 and VI-500 spectrometers using deuterochloroform ($CDCl_3$) or deuterated acetone (CD_3COCD_3) as solvents, and TMS as internal reference. Polymer purity was analyzed by HPLC with a Gilson 321 Pump (Middleton, WI) equipped with Jordi Gel DVB 500Å (Bellingham, MA) column and a Gilson Prep-ELS detector. Particle sizes were determined by dynamic light scattering (DLS, NICOMP 380ZLS, Particle Sizing Systems, Santa Barbara, CA). CMCs were determined by surface tension measurement (Sigma 700, KSV Instruments, Helsinki, Finland).

Polymer Synthesis

mPEG2K-OMs

To a solution of mPEG2K-OH (20.33 g, 10.10 mmol) in dichloromethane (DCM, 125 ml) under Ar was syringed triethylamine (Et_3N, 3.50 ml, 25.1 mmol) followed by methanesulfonyl chloride (MsCl, 1.56 ml, 20.1 mmol) and solution stirred at room temperature overnight. After 16 h reaction deemed complete by NMR, and reaction was washed with concentrated ammonium chloride (NH_4Cl_{aq}, 50 ml), dried over magnesium sulfate ($MgSO_4$), and volume reduced to 50 ml under vacuum. Solution was then precipitated with diethylether at 0°C and collected by filtration. Precipitate was resuspended in DCM (200 ml) and washed with concentrated sodium bicarbonate ($NaHCO_{3aq}$, 100 ml) and volume reduced to 10 ml *in vacuo*. Benzene (10 ml) was added and solution frozen in dry ice/acetone bath and dried overnight under vacuum to give 16.17 g (7.730 mmol, 76.6%) fluffy white solid. ^1H NMR (500 MHz,$CDCl_3$): δ 4.39 (m, 2H), 3.82 (t, J=4.8 Hz, 2H), 3.77 (t, J=4.8 Hz, 2H), 3.71–3.61 (m, ~166H), 3.55 (t, J=4.8 Hz, 2H), 3.46 (t, J=4.8 Hz, 2H), 3.38 (s, 3H), 3.09 (s, 3H).

mPEG2K-F_{10}-OH

In a typical reaction, to a flame-dried flask was added mPEG2K-OMs (3.861 g, 1.781 mmol) and HO- F_{10}-OH (2.086 g, 3.711 mmol) under an Ar atmosphere. Solids were dissolved in anhydrous dioxane (25 ml) followed by addition of sodium hydride (NaH, 200 mg, 8.3 mmol), flask fitted with condensor and refluxed under Ar. After 24 h, additional 100 mg NaH added, and reaction continued to reflux for additional 24 h. Reaction was cooled to room temperature and solvent removed *in vacuo*. Residue was taken up in DCM and washed with NH_4Cl_{aq}, then brine, dried over $MgSO_4$, and dried *in vacuo*. Crude product purified by flash chromatography with fluorous silica. Sample was loaded in 70% MeOH/H_2O, eluted until no PEG seen by I_2 visualization, and product eluted with THF. THF removed under vacuum. Solid was then dissolved in DCM (10 ml) and benzene (10 ml), frozen in dry ice-acetone bath and dried overnight under vacuum to yield 1.118 g (0.437 mmol, 24.5%) while solid. ^1H NMR (400 MHz,$CDCl_3$): δ 4.08 (t, J=13.4 Hz, 2H), 4.05 (t, J=13.4 Hz, 2H), 3.80 (m, 4H), 3.71–3.61 (m, ~166H), 3.55 (t, J=4.8 Hz, 2H), 3.46 (t, J=4.8 Hz, 2H), 3.38 (s, 3H). ^{19}F NMR (376 MHz, $CDCl_3$): δ -117.2 (m, 2F), -120.0 (m, 2F), -122.2 (m, 10F), -122.4 (m, 2F), -122.8 (m, 2F), -123.9 (m, 2F).

mPEG2K- F_{10}-DSPE

In a typical reaction, to a flame-dried flask charged with acetonitrile (ACN, 25 ml) was added mPEG2K- F_{10}-OH (2.530 g, 0.989 mmol) along with 4Å powdered molecular sieves (0.50 g). N,N′-disuccidimidyl carbonate (DSC, 2.512 g, 9.806 mmol) was added, flask sealed under Ar, pyridine (2.40 ml, 29.7 mmol) syringed in, and flask stirred for 1.5 h at room temperature. Solution was precipitated with ice-cold ether, filtered, and precipitate collected with warm toluene (45°C). Solvent removed *in vacuo* to yield white solid, which was added to a thick-walled reaction flask along with 1,2-distearoyl-*sn*-glycero-3-phosphoethanolamine (903.1 mg, 1.201 mmol) and DCM (25 ml). Et_3N (420 μl, 3.01 mmol) was syringed in, flask flushed with Ar and quickly sealed and allowed to stir in 80°C oil bath for 25 min. Flask allowed to cool to room temperature, then reaction quenched with acetic acid (AcOH, 170 μl, 2.97 mmol) and solvent removed under vacuum. Purification was accomplished by flash chromatography (10:1 ammoniacal chloroform, $CHCl_3$*NH_3,:MeOH). Product lyophilized from benzene to yield 1.805 g (0.541 mmol, 45.1%) fluffy white powder. ^1H NMR (500 MHz,$CDCl_3$): δ 7.05 (br s, 2H), 5.22 (m, 1H), 4.58 (t, J=14.0 Hz, 2H), 4.39 (dd, J=12.1, 3.2 Hz, 1H) 4.15 (dd, J=12.1, 7.1 Hz, 1H), 4.04 (t, J=14.0 Hz, 2H), 3.97 (m, 4H), 3.78 (m, 2H), 3.71–3.61 (m, ~166H), 3.55 (m, 2H), 3.50 (m, 1H), 3.34 (m, 1H), 3.38 (s, 3H), 3.13 (m, 2H), 2.28 (t, J=7.7 Hz, 2H), 2.27 (t, J=7.7 Hz, 2H), 1.59 (m, 4H), 1.26 (br m, 56H), 0.88 (t, J=6.9 Hz, 6H). ^{19}F NMR (376 MHz, $CDCl_3$): δ -120.0 (m, 2F), -120.3 (m, 2F), -122.1 (m, 8F), -122.4 (m, 4F), -123.7 (m, 2F), -123.8 (m, 2F).

mPEG5K-OMs

In a typical reaction, to a flask of mPEG5K-OH (22.383 g, 3.772 mmol) in DCM (125 ml) under Ar was added Et_3N (1.30 ml, 9.33 mmol) followed by MsCl (600 µl, 7.72 mmol), and flask stirred at room temperature for 24 h. Solution diluted to 500 ml with DCM then washed with NH_4Cl_{aq} (2×300 ml), brine (300 ml), dried over $MgSO_4$, filtered, and solvent removed *in vacuo* to yield 20.60 g (3.426 mmol, 90.8%). ^{1}H NMR (500 MHz, $CDCl_3$): δ 4.39 (m, 2H), 3.82 (t, J=4.8 Hz, 2H), 3.78 (m, 4H), 3.71–3.61 (m, ~440H), 3.56 (m, 2H), 3.50 (m, 2H), 3.38 (s, 3H), 3.09 (s, 3H).

HO- F_{10}-OBn

In a typical reaction, to a solution of HO- F_{10}-OH (17.364 g, 30.897 mmol) in DMF (100 ml) under Ar was added crushed KOH (1.79 g, 31.9 mmol). Benzyl bromide (BnBr, 1.22 ml, 10.3 mmol) was then syringed into flask and solution stirred for 12 h. Reaction was filtered and solvent removed *in vacuo*. Residue taken up in ethyl acetate and washed with saturated ammonium chloride, aqueous layer extracted twice with ethyl acetate, and combined organics volume reduced to minimal under vacuum. Crude solution purified by flash chromatography (hexanes/ethyl acetate, 9:1–3:1) to yield 4.10 g (6.28 mmol, 61.0% based on BnBr). Also recovered was 11.01 g HO- F_{10}-OH (19.59 mmol) as well as 1.68 g BnO- F_{10}-OBn (2.26 mmol). ^{1}H NMR (400 MHz,CD_3COCD_3): δ 7.39 (m, 5H), 5.20 (t, J= 7.2 Hz, 1H), 4.77 (s, 2H), 4.21 (t, J= 14.0 Hz, 2H), 4.19 (td, J= 14.0, 7.2 Hz, 2H). ^{19}F NMR (376 MHz, $CDCl_3$): δ -120.3 (m, 2F), -122.7 (m, 10F), -123.0 (m, 4F), -124.2 (m, 2F), -124.4 (m, 2F).

mPEG5K- F_{10}-OBn

In a typical reaction, to a solution of mPEG5K-OMs (11.319 g, 1.882 mmol) in anhydrous THF (500 ml) was added HO- F_{10}-OBn (3.085 g, 4.731 mmol) followed by sodium hydride (1.0 g, 41 mmol) as THF slurry. Flask was then fitted with a condenser and refluxed for 16 h. Reaction mixture was then quenched with water dropwise and filtered, and solvent was evaporated. Crude solid was purified by column chromatography (DCM/MeOH, 1:0–10:1) to afford 8.01 g (1.22 mmol, 64.6%) of an off-white solid. ^{1}H NMR (500 MHz,$CDCl_3$): δ 7.34 (m, 5H), 4.67 (s, 2H), 4.04 (t, J= 13.5 Hz, 2H), 3.94 (t, J= 13.5 Hz, 2H), 3.78 (m, 4H), 3.70–3.60 (m, ~440H), 3.55 (m, 4H), 3.49 (m, 4H), 3.38 (s, 3H). ^{19}F NMR (376 MHz, $CDCl_3$): δ -119.7 (m, 4F), -122.2 (m, 8F), -122.4 (m, 4F), -123.7 (m, 4F).

mPEG5K- F_{10}-OH

In a typical reaction, mPEG5K- F_{10}-OBn (8.01 g, 1.22 mmol) was dissolved in methanol (250 ml) under Ar atmosphere and 5% Pd/C (512 mg) added and reaction allowed to stir under H_2 (1 atm). After 72 h, reaction was filtered through celite and solvent evaporated. Off-white solid was dissolved in minimal DCM and precipitated with ice cold ether, then dissolved in minimal THF and again precipitated with ice cold ether to afford 7.07 g (1.09 mmol, 89.5%) white solid. ^{1}H NMR (500 MHz,$CDCl_3$): δ 4.07 (t, J= 13.5 Hz, 2H), 4.04 (t, J= 13.5 Hz, 2H), 3.78 (m, 4H), 3.70–3.60 (m, ~440H), 3.55 (m, 4H), 3.49 (m, 4H), 3.38 (s, 3H). ^{19}F NMR (376 MHz, $CDCl_3$): δ -120.1 (m, 2F), -122.2 (m, 8F), -122.4 (m, 4F), -122.6 (m, 2F), -123.9 (m, 4F).

mPEG5K- F_{10}-DSPE

In a typical experiment, mPEG5K- F_{10}-OH (7.06 g, 1.09 mmol) and DSC (2.55 g, 9.95 mmol) were dissolved in anhydrous ACN (50 ml) under Ar atmosphere. Pyridine (3.0 ml, 37.1 mmol) syringed into reaction flask and solution stirred for 1.5 h. Reaction mixture was diluted with ACN (50 ml) and precipitated with ice-cold ether. This solid was quickly dissolved in anhydrous DCM (30 ml) and transferred to thick-walled reaction flask. DSPE (928 mg, 1.24 mmol) was added, followed by Et_3N (300 µl, 2.15 mmol), flask flushed with Ar, sealed, and heated in 85°C oil bath for 30 min. Reaction was filtered through celite, purified by column chromatography ($CHCl_3$*NH_3/MeOH, 10:1) and lyophilized to afford 454 mg (.0623 mmol, 30.4%) white powder. ^{1}H NMR (500 MHz, $CDCl_3$): δ 7.05 (br s, 2H), 5.22 (m, 1H), 4.58 (t, J=14.0 Hz, 2H), 4.39 (dd, J=12.1, 3.2 Hz, 1H) 4.15 (dd, J=12.1, 7.1 Hz, 1H), 4.04 (t, J=14.0 Hz, 2H), 3.97 (m, 4H), 3.78 (m, 2H), 3.71-3.61 (m, ~440H), 3.55 (m, 2H), 3.50 (m, 1H), 3.34 (m, 1H), 3.38 (s, 3H), 3.13 (m, 2H), 2.28 (t, J=7.7 Hz, 2H), 2.27 (t, J=7.7 Hz, 2H), 1.59 (m, 4H), 1.26 (br m, 56H), 0.88 (t, J=6.9 Hz, 6H). ^{19}F NMR (376 MHz, $CDCl_3$): δ -120.1 (m, 2F), -120.3 (m, 2F), -122.1 (m, 8F), -122.3 (m, 4F), -123.7 (m, 2F), -123.8 (m, 2F).

Measurement of Surface Tension

Measurements of surface tension were performed with a KSV Sigma 701 tensiometer (KSV Instruments, Helsinki, Finland) using a roughened platinum rod with a diameter of 1.048 mm and wetted length of 3.248 mm. Prior to each run the rod was submerged in absolute ethanol and then flame-dried until rod was glowing orange-red. After flame-drying, the rod was hung on the instrument and allowed to cool for several minutes. As a control, the surface tension of

double-distilled water (Millipore water) was measured. Polymer solutions, each composed of varying concentrations of polymer, and Millipore water were prepared in the vessel with a diameter of 20 mm and a height of 40 mm. Measurements were made in quadruplet, from lowest to highest polymer concentration, at a constant temperature of 25°C. The average surface tension was plotted against the logarithm of polymer concentration to measure the critical micelles concentration (CMC). The surface excess of nonionic surfactants was calculated using the Gibbs adsorption isotherm:

$$\Gamma_{\max} = -\frac{1}{RT}\left(\frac{\partial\gamma}{\partial \ln C}\right)$$

where Γ_{max} is the surface excess concentration at CMC (mole/m^2), R is the universal gas constant, T is the absolute temperature, γ is the surface tension and C is the surfactant concentration. The minimum area per molecule, A_{min} ($Å^2$), at the interface was calculated as

$$A_{\min} = -\frac{10^{20}}{N_A \Gamma_{\max}}$$

where N_A is the Avogadro number (38).

Preparation of AmB-Loaded Micelles

Micelles were prepared using a solvent evaporation method. AmB stock solution was generated by dissolving AmB in methanol, aided by sonication, at a concentration of 250 μg/mL. Polymer was dissolved in 1 mL of AmB stock solution to achieve a final concentration of 2.4×10^{-3} M. Methanol was evaporated at 65°C under reduced pressure on a rotary evaporator to produce a thin film of AmB and polymer. The thin film was rehydrated with 1 mL of PBS buffer (pH 7.4) heated at 65°C with gentle agitation, and the flask was rotated at room temperature for 10 min. Sample was then filtered through 0.45 μm nylon syringe filters to remove any insoluble precipitate.

Measurement of Core Microviscosity

The relative microviscosity of the micelle core was estimated from the intensity ratio (I_M/I_E) of monomer and excimer emission of 1,3-(1,1′-Dipyrenyl)-propane (P3P) at 376 and 480 nm, respectively, in response to excitation at 333 nm (39–41). P3P was dissolved in chloroform and in amber vials to achieve a final P3P concentration of 2×10^{-7} M. Chloroform was then evaporated and replaced with 3 mL of polymeric micelles solution in PBS buffer (pH 7.4) at a concentration of 2×10^{-4} M. Samples were sonicated at 65°C for an hour and cooled to room temperature for 12 h. Emission spectra were obtained at 22°C on an AMINCO-Bowman Series 2 Luminescence Spectrometer (Thermo Electron Corp., Madison, WI, USA).

Förster Resonance Energy Transfer (FRET) Spectroscopy

Briefly, polymer was dissolved in methanol in 50 mL round-bottom flasks at a 1.7×10^{-4} M concentration. 4.6 μg of $DiOC_{18}(3)$ and 4.4 μg of $DiIC_{18}(3)$ were added to achieve final concentrations of 5 μmol. Methanol was evaporated at 65°C under reduced pressure on a rotary evaporator to produce a thin film of $DiOC_{18}(3)$, $DiIC_{18}(3)$ and polymer. The thin film was rehydrated with 1 mL of PBS buffer (pH 7.4) heated at 65°C with gentle agitation, and the flask was rotated at room temperature for 10 min. Sample was then filtered through 0.45 μm nylon syringe filters to remove any insoluble precipitate. FRET experiment was performed by using AMINCO-Bowman Series 2 Luminescence Spectrometer (Thermo Electron Corp., Madison, WI, USA). The detector high voltage was adjusted for 50% of a maximum output signal. The sample was excited at 484 nm, and emission spectra were measured from 495 to 600 nm. One hundred microliter of the micelle was mixed with 1.9 mL of human serum, and the mixture was incubated at room temperature. Fluorescence emission was measured after vigorous agitation every 20 min for 2 h. To remove baseline noise due to human serum, fluorescence of empty micelles in the presence of human serum was also measured and subtracted from the spectra. The stability change of FRET probes-loaded micelles was monitored by calculating the FRET ratio:

$$\text{FRET ratio} = \frac{I_R}{I_G + I_R}$$

where I_R and I_G are the peak fluorescence intensities of $DiIC_{18}(3)$ and $DiOC_{18}(3)$ at 565 and 501 nm, respectively, at t min in response to excitation at 484 nm. FRET ratio at each time point was normalized to the initial FRET ratio.

Quantification of AmB Loading in Micelles

The content of AmB loaded in the micelle was quantified by reverse phase HPLC. The HPLC system used for quantifying was a Shimadzu prominence HPLC system (Shimadzu, Japan), consisting of a LC-20AT pump, SIL-20 AC HT autosampler, CTO-20 AC column oven and a SPD-M20A diode array detector. A 100-μL aliquot of micelle solution was mixed with 900 μL of methanol, and 10 μL of the mixture was injected into a C8 column (Agilent XDB-C8, 4.6×150 mm), eluting with an isocratic mixture of 90% methanol containing 5% of acetic acid and

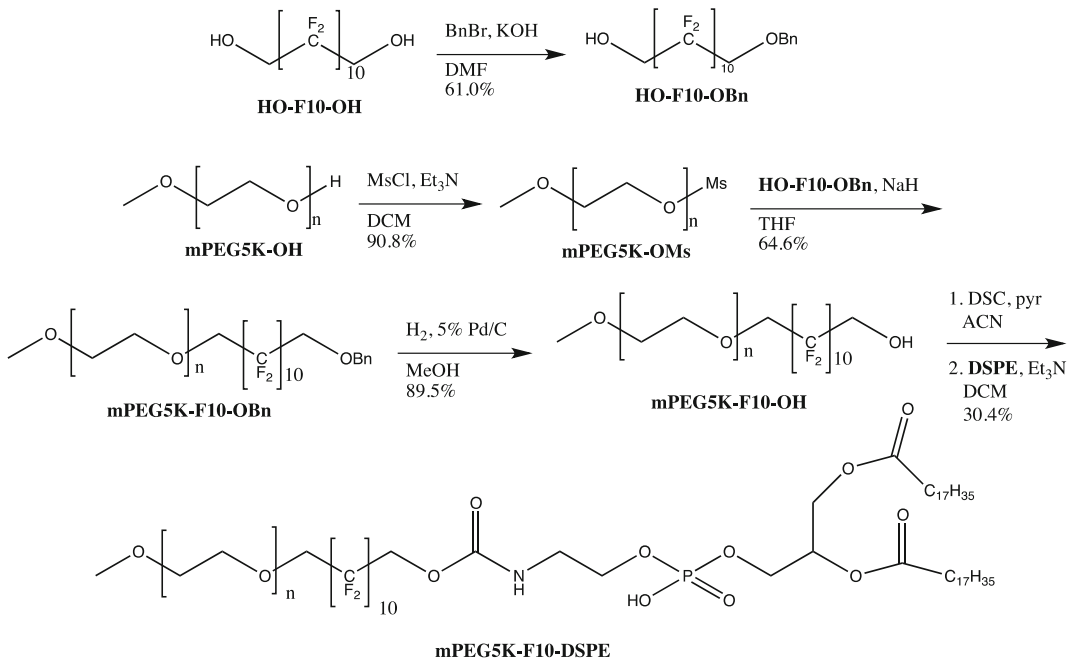

Scheme 1 Synthesis of mPEG5K-F10-DSPE triblock copolymer.

10% Millipore water containing 5% acetic acid. The run time was 3 min, the flow rate was 1.0 mL/min and the detection was at 409 nm. AmB eluted at 1.98 min.

Dynamic Light Scattering (DLS) Measurements of Micelles

Micellar size was determined by dynamic light scattering using a ZETASIZER Nano-ZS Malvern Instruments Inc., Worcestershire, UK) equipped with He-Ne laser (4 mW, 633 nm) light source and 173° angle scattered light collection configuration. Micelle was diluted in Millipore water, and the sample was equilibrated for 2 min at 25°C before measurements. The final polymer concentration was approximately 2.4×10^{-4} M. The hydrodynamic diameter of micelle was calculated based on the Stokes–Einstein equation. Correlation function was curve-fitted by a Cumulants analysis method to calculate mean size and polydispersity index (PDI). All measurements were performed in triplicate, and volume-weighted particle sizes are presented as the average diameter with standard deviation.

In Vitro Release Profiles of AmB from Micelles

The release profile of AmB from micelle was evaluated by a dialysis method. After micelle preparation, each sample was

Scheme 2 Synthesis of mPEG2KF10-DSPE triblock copolymer.

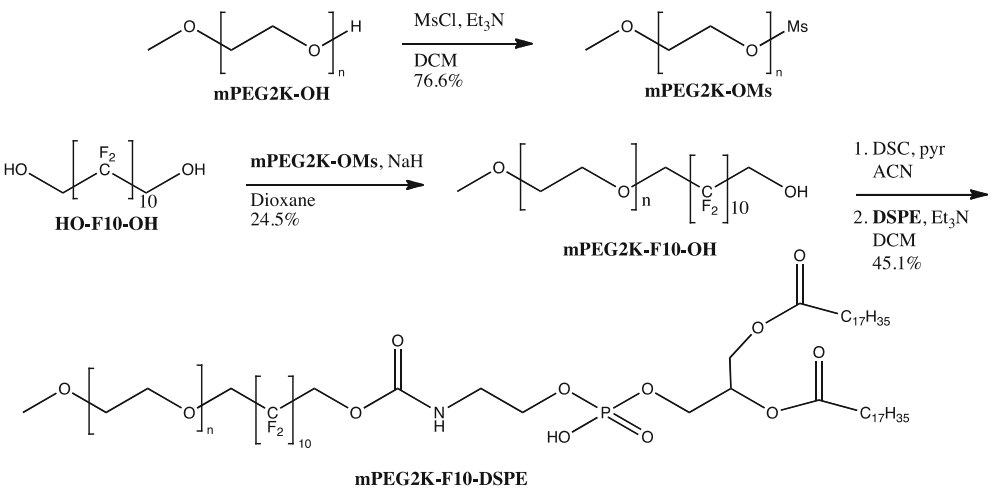

Table I Surface Active Properties of Polymers

Polymer	CMC (M)	γ_{CMC} (mN/m)	$10^6\ \Gamma_{max}$ (mol/m^2)	A_{min} (Å^2)	I_M/I_E	Diameter (nm)
mPEG2K-DSPE	1.38×10^{-5}	57.35	2.12×10^{-6}	78.35	5.69 ± 0.29*	12.44 ± 0.15
mPEG2K-F_{10}-DSPE	8.45×10^{-6}	51.07	5.88×10^{-6}	28.26	9.30 ± 0.38	12.35 ± 0.19
mPEG5K-DSPE	1.40×10^{-4}	55.31	7.67×10^{-7}	217.72	4.89 ± 0.15*	18.62 ± 0.57
mPEG5K-F_{10}-DSPE	2.94×10^{-5}	51.19	1.28×10^{-6}	129.90	7.44 ± 0.42	19.97 ± 0.55

*Denotes statistical significance at $p < 0.05$

diluted with PBS buffer (pH 7.4) for a concentration of 0.2 mg/mL AmB. A volume of 2 mL of the prepared sample was loaded into a 3 mL Slide-A-Lyzer® (Thermo Scientific Inc.) dialysis cassette with a MWCO of 10,000 g/mol. Four cassettes were used in each experiment. The cassettes were placed in 3.0 L of PBS buffer (pH 7.4), which was changed every 3 h until 12 h and then every 12 h until 240 h to ensure sink conditions for AmB and polymer. To prevent drug degradation, 20 μg/mL propyl gallate was added. A sample of 100 μL was drawn from each cassette at various sampling time intervals and then replaced with 100 μL of fresh buffer. The sampling time intervals were 0, 0.5, 2, 3, 6, 9, 12, 24, 36, 48, 72, 96, 120, 144, 168, 192, 216 and 240 h. Curve-fitting analysis using one phase exponential association was used to calculate the half-life ($t_{1/2}$) of drug for *in vitro* drug release experiments. The amount of AmB in each sample was quantified by HPLC as per the "Quantification of AmB Loading in Micelles" section.

Data Analysis

Linear regressions were preformed to calculate CMC. Curve-fitting analysis using one phase exponential association was used to calculate the half-life ($t_{1/2}$) of $DiIC_{18}(3)$ and $DiOC_{18}(3)$ in FRET experiments and AmB in *in vitro* drug release experiments. Comparisons between different sample sets were made using Student's *t*-test. These analyses were performed using GraphPad Prism (version 5.01; GraphPad Software, San Diego, CA, USA).

RESULTS AND DISCUSSION

Polymer Synthesis

The synthetic scheme for mPEG5K- F_{10}-DSPE is shown in Scheme 1. The first step was the monoprotection of the

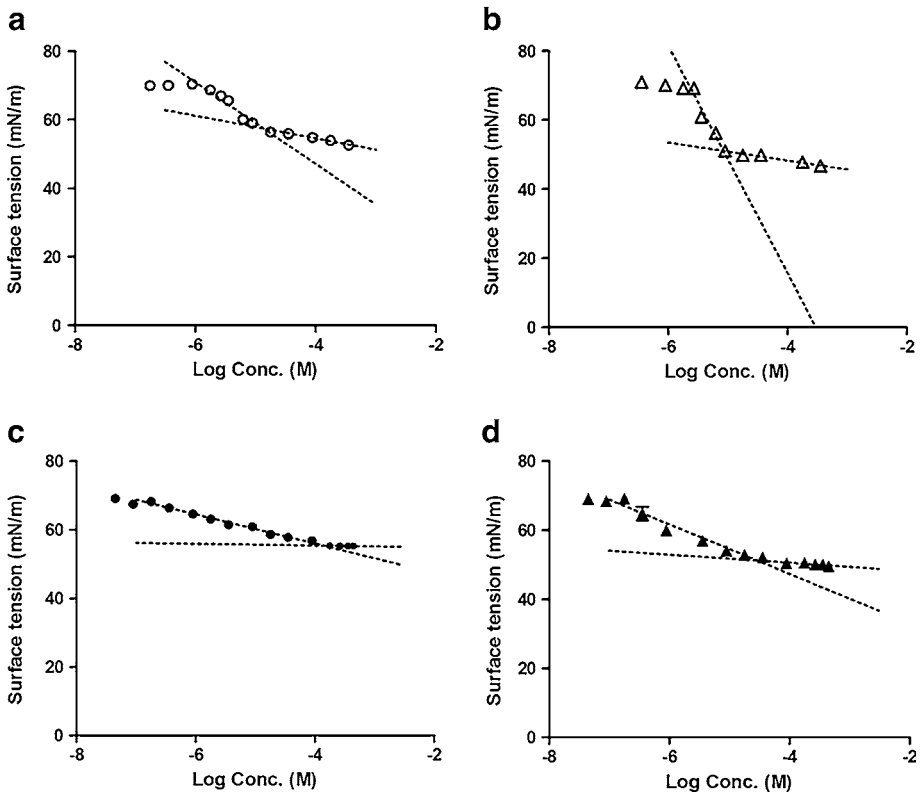

Fig. 1 Surface tensions *versus* log concentration plot for (**a**) mPEG2K-DSPE; (**b**) mPEG2K-F_{10}-DSPE; (**c**) mPEG5K-DSPE; (**d**) mPEG5K-F_{10}-DSPE. The results were expressed as mean ± S.D. ($n = 4$).

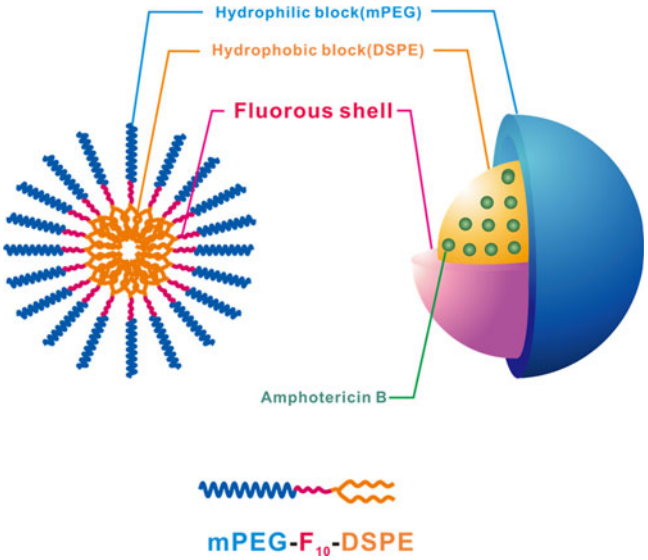

Fig. 2 Schematic representation of AmB-loaded Fluorous shell micelles.

fluorous diol, HO- F_{10}-OH. The rigidity of the fluorous molecule made selective protection impossible; therefore, statistical mono-benzylation was the best route. Due to the higher cost of the fluorous starting material, the most efficient path found was to use a 3:1 ratio of diol to benzyl bromide, giving only a small amount of di-benzylated product. This way, after purification of the desired mono-benzylated molecule, unreacted HO- F_{10}-OH could immediately be recycled and subsequently protected. The di-benzylated product could also be deprotected, purified, and recycled to regenerate the fluorous diol. The PEG mesylate was then made and reacted with HO- F_{10}-OBn and sodium hydride in THF to give the diblock, mPEG5K- F_{10}-OBn. Hydrogenolysis of the benzyl group gave mPEG5K- F_{10}-OH that was then activated with disuccinimidyl carbonate (DSC). To this was added the chosen phospholipid, 1,2-distearoyl-*sn*-glycero-3-phosphoethanolamine (DSPE), forming the carbamate linkage via the primary amine of DSPE to give the tri-block mPEG5K- F_{10}-DSPE. Scheme 2 shows the route beginning with the smaller mPEG2K-OH. When working with the smaller PEG, we found it was more efficient to react mPEG2K-OMs directly with HO- F_{10}-OH without previous mono-benzylation. No significant amount of undesired mPEG- F_{10}-mPEG was found after 48 h, and the product mPEG2K- F_{10}-OH could be purified easily with fluorous silica. This route was not found viable with mPEG5K-OMs, as longer reaction times were required, and significant mPEG5K- F_{10}-mPEG5K was generated and difficult to separate from the desired product. DSPE was then coupled to mPEG2K- F_{10}-OH as with the larger PEG polymer, generating mPEG2K- F_{10}-DSPE.

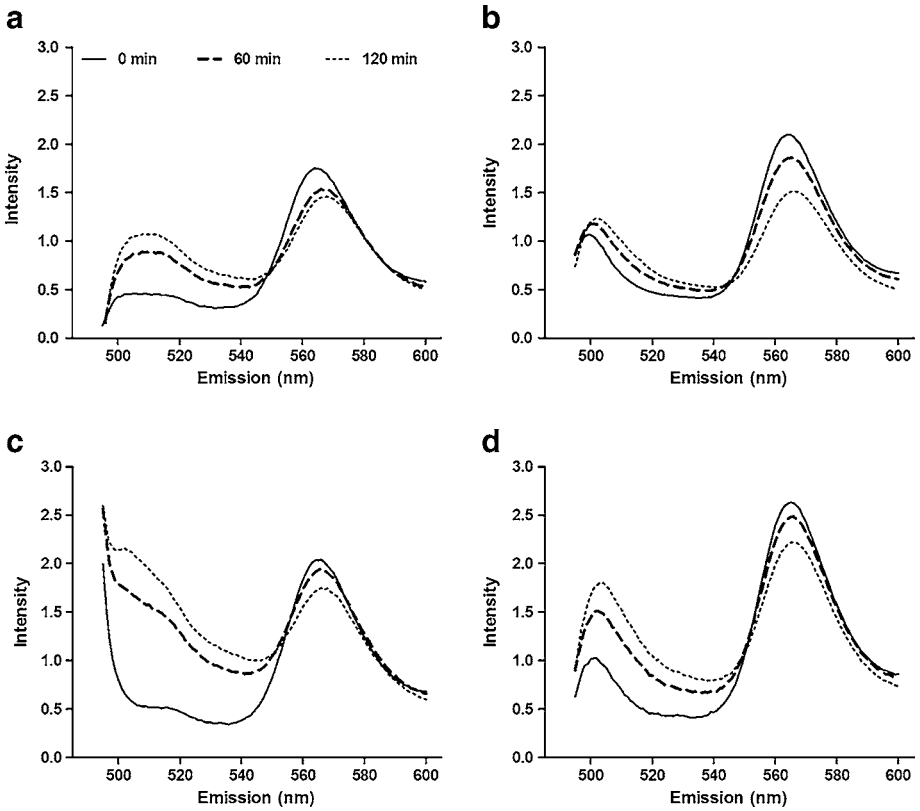

Fig. 3 Fluorescence spectra of $DiIC_{18}(3)$ and $DiOC_{18}(3)$ encapsulated micelles in human serum for 120 min. Fluorescence intensity of (**a**) mPEG2K- DSPE; (**b**) mPEG2K- F_{10}-DSPE; (**c**) mPEG5K-DSPE; (**d**) mPEG5K- F_{10}-DSPE, measured at 22°C.

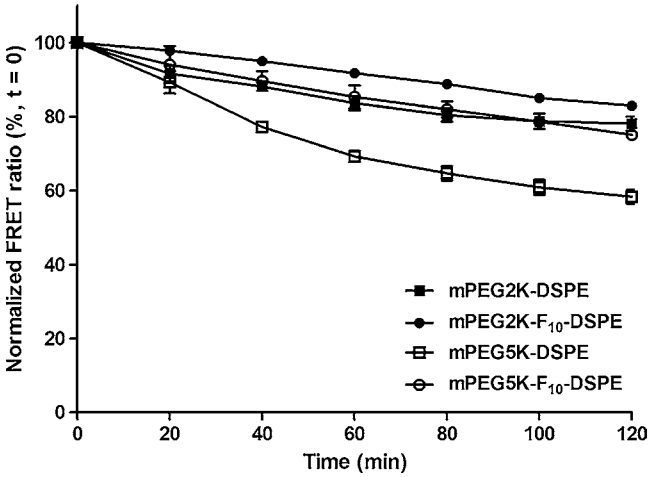

Fig. 4 Normalized FRET ratio of (■) mPEG2K- DSPE; (●) mPEG2K-F_{10}-DSPE; (□) mPEG5K- DSPE; (○) mPEG5K- F_{10}-DSPE, measured over time in human serum for 120 min at 22°C. The results were expressed as mean ± S.D. ($n = 3$).

Determination of CMC

The CMCs of polymers were determined by the surface tension method. The surface tension of a polymer solution was plotted *versus* logarithm of the polymer concentration in Millipore water from which the CMC of the polymer was calculated. The curves used for CMC determination of polymers are given in Fig. 1, and the CMCs of polymers in aqueous solution are presented in Table I. Increasing the length of the hydrophilic PEG block increases the CMC by decreasing the proportion of hydrophobic block of the polymer, consistent with other researchers' results (4,38,42–44). The addition of the center fluorocarbon, as in mPEG2K-F_{10}-DSPE and mPEG5K-F_{10}-DSPE, decreased the CMC relative to the corresponding polymer without fluorocarbons mPEG2K-DSPE and mPEG5K-DSPE, respectively. This increased stability was due to the fluorophilic nature of the fluorous polymers. The fluorocarbons are considerably 1.5 times more hydrophobic than the same numbers of hydrocarbons, and fluorinated amphiphilic polymers are known to exhibit CMCs lower than those of their hydrocarbon analogues (38,45–47). Furthermore, it is reported that the formation of micelles is controlled mainly by the nature of the hydrophobic block not the hydrophilic block (42). The inclusion of a fluorophilic block lowers the CMC, thus increasing the thermodynamic stability of the polymeric micelles.

Determination of Surface Active Properties

To evaluate the surface active properties of the polymers, γ_{CMC}, Γ_{max} and A_{min} were calculated based on the surface tension measurement results (Table I). γ_{CMC} is the limit surface tension of the polymer at its CMC. The γ_{CMC} of mPEG2K-DSPE was higher than that of mPEG2K-F_{10}-DSPE, and the γ_{CMC} of mPEG5K-DSPE was higher than that of mPEG5K-F_{10}-DSPE. The results are in good agreement with other researchers' findings, as γ_{CMC} has been shown to decrease with increasing polymer fluorophilicity due to a higher order packing ratio of the fluorocarbon layer at the air/water interface (38,47). Γ_{max} is the surface excess concentration at the CMC, and A_{min} (Å ^{2}) is the minimum area per molecule. They were obtained from the slope of the surface tension curves. For a given hydrophilic part (mPEG2K or mPEG5K, for instance), Γ_{max} increased and A_{min} decreased when the hydrophobic chain (fluorocarbon) length increased, whereas for a given hydrophobic part (DSPE or F_{10}-DSPE), the opposite trend was obviously observed when the hydrophilic chain length increased. mPEG2K-F_{10}-DSPE had the highest Γ_{max} and the lowest A_{min}. In other words, the fluorophilicity of the polymer affects the surface active properties. These results indicate that as the surfactant molecules become more fluorophilic, the tendency of those molecules to move from the water to the air/water interface is stronger, resulting in a more packed surface and lower CMC (47,48).

Characterization of Micelles Properties

The mean diameters for mPEG2K-DSPE, mPEG2K-F_{10}-DSPE, mPEG5K-DSPE and mPEG5K-F_{10}-DSPE micelles as determined using DLS are listed in Table I. As expected, the diameter of the micelles increased with an increase in hydrophilic chain length (4). However, the introduction of fluorocarbons into the polymers had almost no effect on the micelle's diameter.

P3P, a hydrophobic fluorescent probe, preferentially partitions into the hydrophobic core of micelles. P3P forms

Table II Curve Fit Parameters for FRET Ratio of mPEG2K-DSPE, mPEG2K-F_{10}-DSPE, mPEG5K- DSPE and mPEG5K-F_{10}-DSPE in Human Serum for 120 min at 22°C

Polymer	10^{-3} First-order rate constant (h^{-1})	$t_{1/2}$(h)	Goodness of fit (r^2)
mPEG2K- DSPE	5.16	134.2	0.926
mPEG2K-F_{10}- DSPE	2.99	231.7	0.984
mPEG5K- DSPE	12.9	53.7	0.995
mPEG5K-F_{10}- DSPE	5.11	135.7	0.998

Table III The Mean Diameters of AmB Encapsulated mPEG2K- DSPE, mPEG2K- F_{10}-DSPE, mPEG5K- DSPE and mPEG5K- F_{10}-DSPE Micelles at 0 and 24 h. The Results Were Expressed as Mean ± S.D. ($n = 3$)

Polymer	with 250 μg/mL AmB [a]		
	Diameter (nm)		
	Initial	At 24 h	% changed at 24 h [b]
mPEG2K-DSPE	12.65 ± 0.39	13.10 ± 0.38	4 ± 6
mPEG2K-F_{10}-DSPE	13.69 ± 0.50	13.31 ± 0.61	−3 ± 7
mPEG5K-DSPE	23.02 ± 0.74	23.25 ± 0.44	1 ± 5
mPEG5K-F_{10}-DSPE	22.80 ± 0.94	22.83 ± 1.29	1 ± 5

[a] Solutions were prepared with 250 μg/mL AmB

[b] % changed = (diameter at 24 h-initial diameter)/initial diameter × 100

intramolecular pyrene excimers due to a free rotation of carbon bonds placed between two pyrene fragments when excited. The conformational change in P3P is restricted by core friction proportional to the viscosity of its environment. Therefore, a higher monomer to excimer fluorescent intensity ratio (I_M/I_E) of P3P is evidence of microenvironment viscosity (39–41). For a given hydrophilic block (mPEG2K or mPEG5K, for instance), the I_M/I_E ratio increased with the presence of the fluorocarbon (Table I). Compared to the micelles without the fluorocarbons, the micelles with the fluorocarbons had ca. 66% (mPEG2K-DSPE *vs.* mPEG2K-F_{10}-DSPE) and 52% (mPEG5K-DSPE *vs.* mPEG5K-F_{10}-DSPE), respectively, higher viscous cores. As presented in Fig. 2, the fluorocarbons in the micelles may have formed a shield between the hydrophilic and hydrophobic parts, and the shield restricts the motion of P3P in core and leads to a higher viscosity. For a given hydrophobic part (DSPE or F_{10}-DSPE), the I_M/I_E ratio decreased when the hydrophilic chain length increased. Ashok, B. *et al.* (4) reported that the aggregation number of mPEG2K-DSPE is higher than that of mPEG5K-DSPE. This indicated that mPEG2K-DSPE micelles are composed of more mPEG2K-DSPE molecules than that of mPEG5K-DSPE per a micelle. Fewer molecules of mPEG5K-DSPE per micelle lead to a lower I_M/I_E ratio and less restricted motion in the mPEG5K-DSPE micellar core. mPEG2K-F_{10}-DSPE had the highest I_M/I_E ratio, representing the highest core viscosity and the most restricted motions in the micellar core environment. These results indicated that the fluorocarbon's presence leads to higher core viscosity and may enhance *in vitro* and *in-vivo* stability by retarding disintegration at concentrations lower than CMC.

For a potential *in vivo* application, the delivery system has to be stable in the presence of blood components. To investigate the effect that polymer structure had on the micellar stability in human serum, a FRET experiment was employed with fluorescent, lipophilic acceptor ($DiIC_{18}(3)$) and donor probes ($DiOC_{18}(3)$). When the probes are encapsulated into micelles, the close distance between donor and acceptor probes leads to a strong FRET. FRET efficiency decreases as the distance between donor and acceptor probes increases due to micelle structure changes such as swollenness, dissociation of micelles or release of the encapsulated probes. Therefore, FRET results offer an accurate tool for monitoring micelle stability (8,49). The micellar stability was measured in human serum by

Table IV AmB Encapsulation in Polymeric Micelles at 0 and 24 h. The Results Were Expressed as Mean ± S.D. ($n = 3$)

Polymer	With 250 μg/mL of AmB [a]			
	Initial solubility AmB (μg/mL)	AmB loading efficiency (%)	Solubility AmB at 24 h (μg/mL)	% changed at 24 h [b]
mPEG2K-DSPE	242.14 ± 2.67*	97 ± 1	241.27 ± 1.86	−1 ± 2
mPEG2K-F_{10}-DSPE	249.76 ± 2.06*	100 ± 1	247.27 ± 2.87	−2 ± 1
mPEG5K-DSPE	226.46 ± 2.88**	90 ± 3	217.82 ± 8.67	−4 ± 3
mPEG5K-F_{10}-DSPE	238.56 ± 1.95**	95 ± 1	235.94 ± 8.50	−1 ± 3

[a] Solutions were prepared with 250 μg/mL AmB

[b] % changed = (concentration at 24 h-initial concentration)/initial concentration × 100

*Denotes statistical significance at $p < 0.05$

**Denotes statistical significance at $p < 0.01$

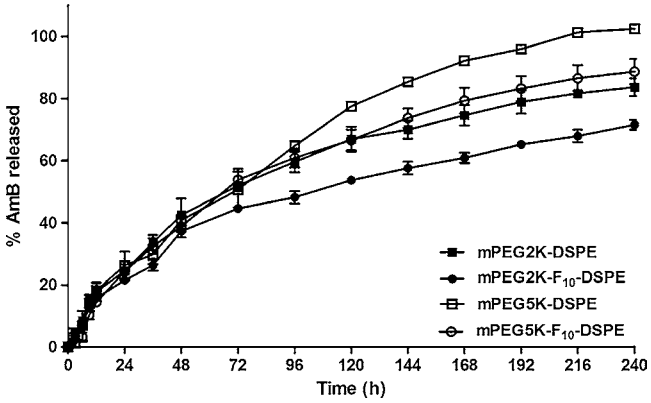

Fig. 5 *In vitro* AmB release kinetics from (■) mPEG2K- DSPE; (●) mPEG2K- F_{10}-DSPE; (□) mPEG5K- DSPE; (○) mPEG5K- F_{10}-DSPE, at 37°C. The results were expressed as mean ± S.D. ($n = 4$).

monitoring time-dependent changes in FRET. Figure 3 presents fluorescence spectra of mPEG2K-DSPE, mPEG2K-F_{10}-DSPE, mPEG5K-DSPE and mPEG5K-F_{10}-DSPE micelles, with encapsulated $DiIC_{18}(3)$ and $DiOC_{18}(3)$, in human serum for 2 h at 22°C. A change in fluorescence spectra over time, specifically increased intensities of $DiOC_{18}(3)$ at 501 nm and decreased intensities of $DiIC_{18}(3)$ at 565 nm, indicated an increased distance between $DiOC_{18}(3)$ and $DiIC_{18}(3)$. Spectra are illustrated in Fig. 4 and summarized in Table II. mPEG5K-DSPE micelles lost FRET efficiency most rapidly, followed by mPEG2K-DSPE and mPEG5K-F_{10}-DSPE micelles, respectively. The highest FRET efficiency remained at ca. 90% in mPEG2K-F_{10}-DSPE micelles after 2 h. The different rates of change in FRET from the micelles correlated with the surface active properties of the polymers such as CMC, minimum area, core viscosity, aggregation number and particle size. For a given hydrophobic block (DSPE or F_{10}-DSPE), the micelles with mPEG5K polymers were less stable than those with mPEG2K polymers. In comparison with the mPEG2K polymers, the mPEG5K polymers had a higher CMC, larger minimum area (A_{min}), larger particle size and lower core viscosity, as previously shown, and these properties correlated to a faster loss of FRET efficiency in human serum. For a given hydrophilic block (mPEG2K or mPEG5K), the micelles with fluorinated polymers better retained the probes in their cores and resulted in higher FRET efficiency than those without fluorocarbons after 2 h. These results suggest that the fluorinated block between hydrophilic and hydrophobic blocks enhances the thermodynamic stability of the micelles in the presence of human serum.

Encapsulation of AmB

Using a simple solvent evaporation method (49,50), AmB was encapsulated into mPEG2K-DSPE, mPEG2K-F_{10}-DSPE, mPEG5K-DSPE and mPEG5K-F_{10}-DSPE micelles. Table III summarizes the sizes of AmB-encapsulated mPEG2K-DSPE, mPEG2K-F_{10}-DSPE, mPEG5K-DSPE and mPEG5K-F_{10}-DSPE micelles at 0 and 24 h as measured by DLS. All micelles exhibited a unimodal distribution with a size range of 15–25 nm. In comparison with the micelles without AmB, the sizes of the micelles increased with the encapsulation of AmB. The sizes of AmB-encapsulated micelles did not significantly change after 24 h storage at 10°C.

The AmB encapsulation concentrations of the micelles at 0 and 24 h are listed in Table IV. mPEG2K-DSPE and mPEG2K-F_{10}-DSPE micelles encapsulated ca. 97% and 100% of initially added AmB, respectively. mPEG5K-DSPE and mPEG5K-F_{10}-DSPE micelles encapsulated ca. 90% and 95% of initially added AmB, respectively. Significantly more AmB was encapsulated into the micelles with shorter chain length of mPEG. Ashok, B. *et al.* (4) similarly reported that longer PEG chain of PEG-DSPE micelles encapsulate less diazepam. Longer mPEG chain length of the polymer may have adversely affected AmB encapsulation into the micelles due to their more static structures. With a given hydrophilic part (mPEG2K or mPEG5K), the micelles with the fluorocarbons (mPEG2K-F_{10}-DSPE and mPEG5K-F_{10}-DSPE) encapsulated significantly more AmB than those without. Fluorocarbons are more hydrophobic than the corresponding hydrocarbons containing the same number of carbon atoms; however, fluorocarbons are considerably lipophobic and strongly incompatible with hydrocarbons (12,16,17,41,51). Preliminary work in our group failed to encapsulate AmB into a fluorous micellar core of related block co-polymers (data not shown), indicating that the fluorocarbons of the micelles did not interact directly with AmB, but the fluorinated shell protected the AmB against loss from the core in the encapsulation process. The different structures of the polymers resulted in different encapsulation amount of

Table V Curve Fit Parameters for *In Vitro* AmB Release from (■) mPEG2K- DSPE; (●) mPEG2K-F_{10}-DSPE; (□) mPEG5K- DSPE; (○) mPEG5K- F_{10}-DSPE, at 37°C

Polymer	10^{-3} First-order rate constant (h^{-1})	$t_{1/2}$(h)	Goodness of fit (r^2)
mPEG2K- DSPE	9.28	74.73	0.980
mPEG2K-F_{10}- DSPE	6.35	109.20	0.952
mPEG5K- DSPE	12.30	56.60	0.985
mPEG5K-F_{10}- DSPE	9.77	70.98	0.993

AmB, but once AmB was encapsulated the AmB was retained in the micelles for 24 h at 10°C.

In Vitro Release Profiles of AmB from Different Micelles

To investigate the *in vitro* release kinetics of AmB from AmB-encapsulated micelles, each micelle solution was dialyzed against excess PBS buffer (49). mPEG2K-F_{10}-DSPE, mPEG2K-DSPE, mPEG5K-F_{10}-DSPE and mPEG5K-DSPE micelles released ca. 72%, 84%, 89% and 100% of AmB for 240 h, respectively (Fig. 5). The *in vitro* drug release data was curve fitted by one phase exponential association, which was then used to calculate the first-order rate constant, $t_{1/2}$, of AmB release from the micelles and the goodness of fit. As presented in Table V, AmB was released with the slowest rate ($t_{1/2}$ of 109.2 h) from mPEG2K-F_{10}-DSPE micelles, which also had the lowest CMC, had the highest core viscosity and was the most stable in human serum. AmB was released with the fastest rate ($t_{1/2}$ of 56.6 h) from mPEG5K-DSPE micelles, which had the highest CMC, had the lowest core viscosity and dissociated with the fastest rate in human serum. AmB was released with intermediate rates from mPEG2K-DSPE ($t_{1/2}$ of 74.73 h) and mPEG5K-F_{10}-DSPE micelles ($t_{1/2}$ of 70.98 h), which have intermediate surfactant properties compared to those of mPEG2K-F_{10}-DSPE and mPEG5K-DSPE micelles. Previous studies reported that drug association and interaction with micelles and subsequent release from micelles are dependent on physical and chemical properties of micelles, including CMC, core state and surface state (52–54).

PEG functionalization has been used in several drug delivery systems to reduce protein uptake, interaction with opsonins, and recognition by the reticuloendothelial system (RES) (55–57). For instance, Doxil® (Doxorubicin liposome), which is approved for clinical applications, uses the polymer PEG2K-DSPE to enhance the liposome stability and blood circulation (58). Interestingly, the polymer PEG5K-DSPE, which has a longer PEG moiety, has similar or no additional suppression effect on RES uptake compared to PEG2K-DSPE (3,57). Furthermore, the formulations coated with PEG2K had longer circulation times than those with PEG5K (59,60). These reports are in agreement with our results. The fluorinated shell in the micelles particularly affected the *in vitro* release kinetics of AmB, as polymers containing a fluorous block had significantly longer half-lives than their non-fluorinated analogues. Specifically, the fluorous shell modulated the sustained release of AmB from the hydrophobic core of the micelles, suggesting that the drug release rate can be controlled through the size of the fluorocarbon.

CONCLUSIONS

We have synthesized poly(ethylene glycol)-fluorocarbon-phospholipid triblock copolymers, and we have characterized their physicochemical and drug release properties. Comparison with the analogous polymers that do not contain the intermediate fluorocarbon block showed that the micelles with the polymers bearing the fluorocarbons have lower CMCs, preferable surface active properties contributing to micellar stability, and higher micelle-core viscosity. The fluorinated shell in the micellar structures induces enhanced thermodynamic stability of the micelles in presence of human serum and allows sustained release of Amphotericin B from the micelles. Micelle stability, drug release rates and pharmacokinetic behavior can be modulated through the size of the fluorocarbon introduced in the polymer.

ACKNOWLEDGMENTS & DISCLOSURES

The authors would like to thank Dr. Glen S. Kwon and Thomas A. Diezi, University of Wisconsin, for technical advice and thoughtful suggestions. This project was supported in part by NIH (GM079375) and NSF (CHE 0518112) to SM. We also thank the University of Wisconsin-Madison School of Pharmacy for support. JPJ acknowledges support from the Korean Research Foundation (KRF-2008-357-E00065).

REFERENCES

1. Singh S, Dash AK. Paclitaxel in cancer treatment: perspectives and prospects of its delivery challenges. Crit Rev Ther Drug Carrier Syst. 2009;26(4):333–72.
2. Yoon HJ, Jang WD. Polymeric supramolecular systems for drug delivery. J Mater Chem. 2010;20(2):211–22.
3. Allen TM, Hansen C, Martin F, Redemann C, Yauyoung A. Liposomes containing synthetic lipid derivatives of poly(ethylene glycol) show prolonged circulation half-lives invivo. Biochim Biophys Acta. 1991;1066(1):29–36.
4. Ashok B, Arleth L, Hjelm RP, Rubinstein I, Onyuksel H. *In vitro* characterization of PEGylated phospholipid micelles for improved drug solubilization: effects of PEG chain length and PC incorporation. J Pharm Sci. 2004;93(10):2476–87.
5. Gabizon AA, Barenholz Y, Bialer M. Prolongation of the circulation time of doxorubicin encapsulated in liposomes containing a polyethylene glycol-derivatized phospholipid—pharmacokinetic studies in rodents and dogs. Pharm Res. 1993;10(5):703–8.
6. Lukyanov AN, Torchilin VP. Micelles from lipid derivatives of water-soluble polymers as delivery systems for poorly soluble drugs. Adv Drug Deliv Rev. 2004;56(9):1273–89.
7. Torchilin VP. Structure and design of polymeric surfactant-based drug delivery systems. J Control Release. 2001;73(2–3):137–72.
8. Chen H, Kim S, He W, Wang H, Low PS, Park K, *et al.* Fast release of lipophilic agents from circulating PEG-PDLLA micelles revealed by *in vivo* Forster resonance energy transfer imaging. Langmuir. 2008;24(10):5213–7.

9. Savic R, Azzam T, Eisenberg A, Maysinger D. Assessment of the integrity of poly(caprolactone)-b-poly(ethylene oxide) micelles under biological conditions: a fluorogenic-based approach. Langmuir. 2006;22(8):3570–8.
10. Xu XY, Zhang XF, Wang XH, Li YX, Jing XB. Comparative study of paclitaxel physically encapsulated in and chemically conjugated with PEG-PLA. Polym Adv Technol. 2009;20(11):843–8.
11. Bae KH, Lee Y, Park TG. Oil-encapsulating PEO-PPO-PEO/PEG shell cross-linked nanocapsules for target-specific delivery of paclitaxel. Biomacromolecules. 2007;8(2):650–6.
12. O'Reilly RK, Hawker CJ, Wooley KL. Cross-linked block copolymer micelles: functional nanostructures of great potential and versatility. Chem Soc Rev. 2006;35(11):1068–83.
13. Shuai XT, Merdan T, Schaper AK, Xi F, Kissel T. Core-cross-linked polymeric micelles as paclitaxel carriers. Bioconjug Chem. 2004;15(3):441–8.
14. Xu YM, Meng FH, Cheng R, Zhong ZY. Reduction-sensitive reversibly crosslinked biodegradable micelles for triggered release of doxorubicin. Macromol Biosci. 2009;9(12):1254–61.
15. Tian L, Yam L, Wang JZ, Tat H, Uhrich KE. Core crosslinkable polymeric micelles from PEG-lipid amphiphiles as drug carriers. J Mater Chem. 2004;14(14):2317–24.
16. Kiss LE, Kovesdi I, Rabai J. An improved design of fluorophilic molecules: prediction of the ln P fluorous partition coefficient, fluorophilicity, using 3D QSAR descriptors and neural networks. J Fluor Chem. 2001;108(1):95–109.
17. Riess JG. Highly fluorinated amphiphilic molecules and self-assemblies with biomedical potential. Curr Opin Colloid Interface Sci. 2009;14(5):294–304.
18. Wolfson MR, Greenspan JS, Shaffer TH. Pulmonary administration of vasoactive substances by perfluorochemical ventilation. Pediatrics. 1996;97(4):449–55.
19. Kent KM, Cleman MW, Cowley MJ, Forman MB, Jaffe CC, Kaplan M, *et al.* Reduction of myocardial-ischemia during percutaneous transluminal coronary angioplasty with oxygenated fluosol. Am J Cardiol. 1990;66(3):279–84.
20. Spahn DR, van Brempt R, Theilmeier G, Reibold JP, Welte M, Heinzerling H, *et al.* European perflubron emulsion study, G., Perflubron emulsion delays blood transfusions in orthopedic surgery. Anesthesiology. 1999;91(5):1195–208.
21. Krafft MP. Fluorocarbons and fluorinated amphiphiles in drug delivery and biomedical research. Adv Drug Deliv Rev. 2001;47(2–3):209–28.
22. Janjic JM, Ahrens ET. Fluorine-containing nanoemulsions for MRI cell tracking. Wiley Interdiscip Rev Nanomed Nanobiotechnol. 2009;1(5):492–501.
23. Shao K, Huang RQ, Li JF, Han LA, Ye LY, Lou JN, *et al.* Angiopep-2 modified PE-PEG based polymeric micelles for Amphotericin B delivery targeted to the brain. J Control Release. 2010;147(1):118–26.
24. Vakil R, Knilans K, Andes D, Kwon GS. Combination antifungal therapy involving Amphotericin B, rapamycin and 5-fluorocytosine using PEG-phospholipid micelles. Pharm Res. 2008;25(9):2056–64.
25. Vakil R, Kwon GS. Effect of cholesterol on the release of Amphotericin B from PEG-Phospholilpid micelles. Mol Pharm. 2008;5(1):98–104.
26. Gallis HA, Drew RH, Pickard WW. Amphotericin-B - 30 years of clinical-experience. Rev Infect Dis. 1990;12(2):308–29.
27. Girois SB, Chapuis F, Decullier E, Revol BGP. Adverse effects of antifungal therapies in invasive fungal infections: review and meta-analysis. Eur J Clin Microbiol Infect Dis. 2005;24(2):119–30.
28. Barwicz J, Tancrede P. The effect of aggregation state of amphotericin-B on its interactions with cholesterol- or ergosterol-containing phosphatidylcholine monolayers. Chem Phys Lipids. 1997;85(2):145–55.
29. Brajtburg J, Bolard J. Carrier effects on biological activity of Amphotericin B. Clin Microbiol Rev. 1996;9(4):512–31.
30. Bolard J, Legrand P, Heitz F, Cybulska B. One-sided action of amphotericin-B on cholesterol-containing membranes is determined by its self-association in the medium. Biochemistry. 1991;30(23):5707–15.
31. Gruda I, Dussault N. Effect of the aggregation state of Amphotericin-B on its interaction with ergosterol. Biochem Cell Biol-Biochimie Biol Cell. 1988;66(3):177–83.
32. Groll AH, Giri N, Petraitis V, Petraitiene R, Candelario M, Bacher JS, *et al.* Comparative efficacy and distribution of lipid formulations of Amphotericin B in experimental Candida albicans infection of the central nervous system. J Infect Dis. 2000;182(1):274–82.
33. Imhof A, Walter RB, Schaffner A. Continuous infusion of escalated doses of Amphotericin B deoxycholate: an open-label observational study. Clin Infect Dis. 2003;36(8):943–51.
34. Eriksson U, Seifert B, Schaffner A. Comparison of effects of Amphotericin B deoxycholate infused over 4 or 24 hours: randomised controlled trial. Br Med J. 2001;322(7286):579–82.
35. Peleg AY, Woods ML. Continuous and 4 h infusion of Amphotericin B: a comparative study involving high-risk haematology patients. J Antimicrob Chemother. 2004;54(4):803–8.
36. Hiemenz JW. Amphotericin B deoxycholate administered by continuous infusion: does the dosage make a difference? Clin Infect Dis. 2003;36(8):952–3.
37. Bates DW, Su L, Yu DT, Chertow GM, Seger DL, Gomes DRJ, *et al.* Mortality and costs of acute renal failure associated with Amphotericin B therapy. Clin Infect Dis. 2001;32(5):686–93.
38. Abla M, Durand G, Pucci B. Glucose-based surfactants with hydrogenated, fluorinated, or hemifluorinated tails: synthesis and comparative physical-chemical characterization. J Org Chem. 2008;73(21):8142–53.
39. Lavasanifar A, Samuel J, Kwon GS. The effect of alkyl core structure on micellar properties of poly(ethylene oxide)-block-poly(L-aspartamide) derivatives. Colloids Surf B Biointerfaces. 2001;22(2):115–26.
40. Winnik FM. Photophysics of preassociated pyrenes in aqueous polymer-solutions and in other organized media. Chem Rev. 1993;93(2):587–614.
41. Vakil R, Kwon GS. Poly(ethylene glycol)-b-poly(epsilon-caprolactone) and PEG-phospholipid form stable mixed micelles in aqueous media. Langmuir. 2006;22(23):9723–9.
42. Kim SY, Shin ILG, Lee YM, Cho CS, Sung YK. Methoxy poly(ethylene glycol) and epsilon-caprolactone amphiphilic block copolymeric micelle containing indomethacin. II. Micelle formation and drug release behaviours. J Control Release. 1998;51(1):13–22.
43. Francis MF, Lavoie L, Winnik FM, Leroux JC. Solubilization of cyclosporin A in dextran-g-polyethyleneglycolalkyl ether polymeric micelles. Eur J Pharm Biopharm. 2003;56(3):337–46.
44. Jeong YI, Cheon JB, Kim SH, Nah JW, Lee YM, Sung YK, *et al.* Clonazepam release from core-shell type nanoparticles *in vitro*. J Control Release. 1998;51(2–3):169–78.
45. Riess JG. Fluorous micro- and nanophases with a biomedical perspective. Tetrahedron. 2002;58(20):4113–31.
46. Sadtler VM, Giulieri F, Krafft MP, Riess JG. Micellization and adsorption of fluorinated amphiphiles: questioning the 1CF(2)approximate to 1.5CH(2) rule. Chemistry-a European Journal. 10;4:1952–6.
47. Kissa E. Fluorinated surfactants: synthesis, properties, applications, vol. 50. New York: M. Dekker; 1994.
48. Graciani MD, Rodriguez A, Munoz M, Moya ML. Micellar solutions of sulfobetaine Surfactants in water-ethylene glycol mixtures: surface tension, fluorescence, spectroscopic, conductometric, and kinetic studies. Langmuir. 2005;21(16):7161–9.
49. Diezi TA, Bae Y, Kwon GS. Enhanced stability of PEG-block-poly(N-hexyl stearate L-aspartamide) Micelles in the Presence of Serum Proteins. Mol Pharm. 2010;7(4):1355–60.

50. Vakil R, Kwon GS. PEG-phospholipid micelles for the delivery of Amphotericin B. J Control Release. 2005;101(1–3):386–9.
51. Mukerjee P. Fluorocarbon hydrocarbon interactions in micelles and other lipid assemblies, at interfaces, and in solutions. Colloid Surface Physicochem Eng Aspect). 1994;84(1):1–10.
52. Soo PL, Luo LB, Maysinger D, Eisenberg A. Incorporation and release of hydrophobic probes in biocompatible polycaprolactone-block-poly(ethylene oxide) micelles: implications for drug delivery. Langmuir. 2002;18(25):9996–10004.
53. Shuai XT, Ai H, Nasongkla N, Kim S, Gao JM. Micellar carriers based on block copolymers of poly(e-caprolactone) and poly(ethylene glycol) for doxorubicin delivery. J Contr Release. 2004;98(3):415–26.
54. Forrest ML, Won CY, Malick AW, Kwon GS. *In vitro* release of the mTOR inhibitor rapamycin from poly(ethylene glycol)-b-poly (epsilon-caprolactone) micelles. J Contr Release. 2006;110(2):370–7.
55. Lasic DD, Martin FJ. Stealth liposomes. Boca Raton: CRC; 1995.
56. Torchilin VP, Shtilman MI, Trubetskoy VS, Whiteman K, Milstein AM. Amphiphilic vinyl-polymers effectively prolong liposome circulation time *in-vivo*. Biochim Biophys Acta-Biomembr. 1994;1195(1):181–4.
57. Lukyanov AN, Gao ZG, Mazzola L, Torchilin VP. Polyethylene glycol-diacyllipid micelles demonstrate increased acculumation in subcutaneous tumors in mice. Pharm Res. 2002;19(10):1424–9.
58. Gabizon A, Shmeeda H, Barenholz Y. Pharmacokinetics of pegylated liposomal doxorubicin - Review of animal and human studies. Clin Pharmacokinet. 2003;42(5):419–36.
59. Maruyama K, Yuda T, Okamoto A, Ishikura C, Kojima S, Iwatsuru M. Effect of molecular-weight in amphipathic poly-ethyleneglycol on prolonging the circulation time of large unilamellar liposomes. Chem Pharm Bull. 1991;39(6):1620–2.
60. Liu F, Liu D. Long-circulating emulsions (oil-in-water) as carriers for lipophilic drugs. Pharm Res. 1995;12(7):1060–4.